JACS
JOURNAL OF THE AMERICAN CHEMICAL SOCIETY
Article
pubs.acs.org/JACS

Spectroscopic and Electrochemical Characterization of the Iron–Sulfur and Cobalamin Cofactors of TsrM, an Unusual Radical *S*-Adenosylmethionine Methylase

Anthony J. Blaszczyk,[†] Alexey Silakov,[*,‡] Bo Zhang,[‡] Stephanie J. Maiocco,[§] Nicholas D. Lanz,[†] Wendy L. Kelly,[∥] Sean J. Elliott,[*,§] Carsten Krebs,[*,†,‡] and Squire J. Booker[*,†,‡,⊥]

[†]Department of Biochemistry and Molecular Biology and [‡]Department of Chemistry and [⊥]Howard Hughes Medical Institute, The Pennsylvania State University, University Park, Pennsylvania 16802, United States

[§]Department of Chemistry, Boston University, 590 Commonwealth Avenue, Boston, Massachusetts 02215, United States

[∥]School of Chemistry and Biochemistry and the Parker H. Petit Institute for Bioengineering and Bioscience, Georgia Institute of Technology, Atlanta, Georgia 30332, United States

Supporting Information

ABSTRACT: TsrM, an annotated radical *S*-adenosylmethionine (SAM) enzyme, catalyzes the methylation of carbon 2 of the indole ring of L-tryptophan. Its reaction is the first step in the biosynthesis of the unique quinaldic acid moiety of thiostrepton A, a thiopeptide antibiotic. The appended methyl group derives from SAM; however, the enzyme also requires cobalamin and iron–sulfur cluster cofactors for turnover. In this work we report the overproduction and purification of TsrM and the characterization of its metallocofactors by UV–visible, electron paramagnetic resonance, hyperfine sublevel correlation (HYSCORE), and Mössbauer spectroscopies as well as protein-film electrochemistry (PFE). The enzyme contains 1 equiv of its cobalamin cofactor in its as-isolated state and can be reconstituted with iron and sulfide to contain one [4Fe–4S] cluster with a site-differentiated Fe^{2+}/Fe^{3+} pair. Our spectroscopic studies suggest that TsrM binds cobalamin in an uncharacteristic five-coordinate base-off/His-off conformation, whereby the dimethylbenzimidazole group is replaced by a non-nitrogenous ligand, which is likely a water molecule. Electrochemical analysis of the protein by PFE indicates a one-electron redox feature with a midpoint potential of −550 mV, which is assigned to a $[4Fe–4S]^{2+}/[4Fe–4S]^{+}$ redox couple. Analysis of TsrM by Mössbauer and HYSCORE spectroscopies suggests that SAM does not bind to the unique iron site of the cluster in the same manner as in other radical SAM (RS) enzymes, yet its binding still perturbs the electronic configuration of both the Fe/S cluster and the cob(II)alamin cofactors. These biophysical studies suggest that TsrM is an atypical RS enzyme, consistent with its reported inability to catalyze formation of a 5′-deoxyadenosyl 5′-radical.

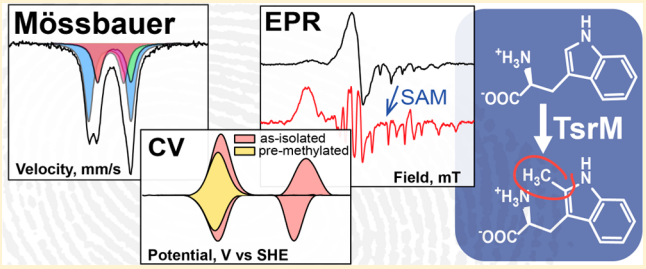

INTRODUCTION

The methylation of unactivated C–H bonds is a burgeoning area of mechanistic enzymology, and bioinformatics analyses suggest that these reactions are catalyzed exclusively by radical *S*-adenosylmethionine (SAM) enzymes.[1−4] Radical SAM (RS) methylases catalyze key steps in the biosynthesis of bacteriochlorophyll,[5] pactamycin (antitumor antibiotic),[4] mitomycin C (antitumor agent),[6] moenomycin A (phosphoglycolipid antibiotic),[7] fosfomycin (broad-spectrum antibiotic),[8−11] thienamycin (β-lactam antibiotic),[12,13] gentamicin (aminoglycoside antibiotic),[14] clorobiocin (aminocoumarin antibiotic),[15] fortimicin (aminoglycoside antibiotic),[16,17] thiostrepton (thiopeptide antibiotic),[18] and chondrochloren (antibiotic),[19] among many other natural products. An enzyme in the biosynthesis of bialaphos (herbicide)[20,21] is also in this family, although it catalyzes methylation of a phosphorus atom rather than a carbon atom. In addition to SAM, a subset of these enzymes, termed Class B RS methylases, are predicted to bind cobalamin, and several have been shown to do so experimentally.[22,23]

TsrM, a Class B RS methylase, catalyzes the first step in the biosynthesis of the quinaldic acid moiety of the thiopeptide antibiotic, thiostrepton, which is the methylation of C2 of the indole ring of L-tryptophan (Trp) (Figure 1).[24] The appended methyl group derives from SAM; however, metabolic feeding studies using chirally labeled methionine indicate that the attachment of the methyl group takes place with overall

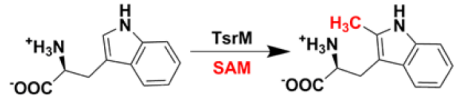

Figure 1. Methylation of C2 of tryptophan catalyzed by TsrM.

Received: December 2, 2015
Published: February 3, 2016

DOI: 10.1021/jacs.5b12592
J. Am. Chem. Soc. 2016, 138, 3416–3426

retention of configuration.[25] This observation contrasts with the established paradigm for SAM-dependent methyl transfer reactions, which proceed by S_N2 attack,[26,27] and therefore with inversion of configuration, but can be rationalized by the finding that the cobalamin cofactor acts as an intermediate methyl carrier between SAM and the methylated product.[28] Although the transfer of the methyl group from SAM to the cobalamin cofactor almost certainly takes place by S_N2 attack of a cob(I)alamin species onto SAM's methyl group, the mechanism by which methylcobalamin transfers the methyl group to tryptophan is unknown.

RS enzymes share distinguishing features within their primary structures, and almost all catalyze a reductive fragmentation of SAM to generate a 5′-deoxyadenosyl 5′-radical (5′-dA•). The 5′-dA• has been thought to be a common intermediate in all family members, which abstracts target hydrogen atoms (H atoms) from enzyme-bound substrates.[29] SAM cleavage requires a low-potential reductant that reduces a $[4Fe-4S]^{2+}$ cluster to the $[4Fe-4S]^{+}$ state. In vivo, the flavodoxin/flavodoxin reductase/NADPH reducing system can supply the necessary electron in many organisms, while in vitro, chemical reductants such as dithionite, reduced methyl viologen, or illuminated deazaflavin are routinely used.[30] In most characterized RS enzymes, the cleavage of SAM is irreversible and one or more equivalents of 5′-deoxyadenosine (5′-dA) are generated per equivalent of product. In a small subset of RS enzymes, SAM is reformed at the end of each catalytic cycle.[30,31]

Recent studies of five Class B RS methylases suggest that, although each requires cobalamin for turnover, their mechanisms of catalysis may be distinctly different.[23] For example, Fom3, PhpK, ThnK, and GenK all catalyze methylation of an sp^3-hybridized atom (carbon atoms for Fom3, ThnK, and GenK, and a phosphorus atom for PhpK) in the presence of cobalamin, SAM, and a low-potential reductant; however, 5′-dA was only observed in the ThnK and GenK reactions.[13,32−34] In contrast to these RS methylases, TsrM uses cobalamin to catalyze the methylation of an sp^2-hybridized carbon center. However, despite showing that TsrM has the ability to catalyze multiple turnovers in 1 h, a previous study reported that no 5′-dA was generated. Moreover, in contrast to most RS enzymes, which require a low-potential reductant to effect cleavage of SAM, TsrM catalyzed multiple turnovers even when dithiothreitol (DTT) was present as the sole reductant.[28]

These anomalies, as well as our general interest in understanding mechanisms by which sp^2-hybridized carbon centers are functionalized, led us to study TsrM in more detail. We report the first isolation of a Class B RS methylase that is fully reconstituted with its cobalamin cofactor, which exists in cob(I)alamin, cob(II)alamin, and presumably cob(III)alamin states. We show that the cob(II)alamin form of the cofactor is five-coordinate, but is neither coordinated axially by its benzimidazole group (base-off) nor coordinated axially by any other nitrogen-containing atom such as from a histidine residue. Upon addition of SAM, the five-coordinate species converts into one that is possibly pseudo four-coordinate, wherein a coordinating molecule, most likely water, or becomes loosely coordinated to the cobalt ion. Interestingly, analysis of the protein by Mössbauer and hyperfine sublevel correlation (HYSCORE) spectroscopies suggests that the unique iron ion of the iron−sulfur (Fe/S) cluster is bound by an unidentified molecule that is neither SAM nor methionine. Moreover, although SAM binding causes changes in the electronic configuration of the Fe/S and cobalamin cofactors, it either does not bind directly to the Fe/S cluster or does not bind to the Fe/S cluster in the fashion that is typical for RS enzymes. Despite these differences, our electrochemical characterization of the Fe/S cluster by protein film electrochemistry (PFE) indicates that it exhibits a midpoint potential that is similar to that of other [4Fe−4S] clusters in RS enzymes. Collectively, our studies indicate that TsrM is an unusual RS enzyme, consistent with its inability to catalyze a reductive cleavage of SAM to a 5′-dA• under normal turnover conditions.

EXPERIMENTAL SECTION

All DNA-modifying enzymes and reagents were obtained from New England Biolabs (Ipswich, MA). The expression vector pSUMO was purchased from Lifesensors, Inc. (Malvern, PA). The RosettaBlue (DE3) pLysS strain of *E. coli* was purchased from Novagen (Madison, WI). Trp, hydroxocobalamin hydrochloride (OHCbl), L-cysteine (Cys), L-tyrosine (Tyr), *N*-(2-hydroxyethyl)piperazine-*N*′-(2-ethanesulfonic acid) (HEPES), sodium sulfide, 2-mercaptoethanol (BME), ferric chloride, 5′-dA, *S*-adenosyl-L-homocysteine (SAH), deuterium oxide (D_2O) (99.9% D), and sodium dithionite were purchased from Sigma Corp. (St. Louis, MO). Chloramphenicol, DTT, nickel nitrilotriacetic acid (Ni-NTA) resin, and isopropyl β-D-1-thiogalactopyranoside (IPTG), kanamycin, and ampicillin were purchased from Gold Biotechnology (St. Louis, MO). Imidazole was purchased from Alfa Aesar (Ward Hill, MA) and potassium chloride (KCl) was purchased from J.T Baker (Phillipsburg, NJ). Glycerol was purchased from EMD Chemicals Inc. (Gibbstown, NJ). DL-[$^2H_8$]-Tryptophan (Trp-d_8) was purchased from C/D/N Isotopes Inc. (Pointe-Claire, Quebec, Canada). The bovine serum albumin (BSA) standard and Bradford reagent for determination of protein concentration were purchased from Pierce (Rockford, IL). PD-10 prepoured gel-filtration columns were purchased from GE Biosciences (Pittsburgh, PA). Ferric oxide (^{57}Fe, 95.86%) was purchased from Isoflex USA (San Francisco, CA). L-Methionine (Met) (1-^{13}C, 99%) was purchased from Cambridge Isotope Laboratories, Inc. (Tewksbury, MA). 2-Methyltryptophan (MeTrp) was custom synthesized as described previously.[35] Ulp1 was provided by Dr. Craig Cameron (Pennsylvania State University).

General Methods. UV−vis spectra were recorded on a Cary 50 spectrometer from Varian (Walnut Creek, CA) using the WinUV software package to control the instrument. In addition, all UV−vis spectra were measured in an anaerobic cuvette with 1 mL of sample volume. Sonic disruption of *E. coli* was conducted with a 550 sonic dismembrator (Fisher Scientific; Pittsburgh, PA). Size exclusion chromatography was conducted on a HiPrep 16/60 S-200 column using an ÅKTA fast protein liquid chromatography (FPLC) system (GE Biosciences) in a Coy anaerobic chamber (Grass Lake, MI). Sodium dodecyl sulfate-polyacrylamide gel electrophoresis (SDS-PAGE) was conducted as described previously.[36] $^{57}Fe_2O_3$ was incubated overnight at 70 °C with HCl in an anaerobic chamber to generate $^{57}FeCl_3$. The concentration of $^{57}FeCl_3$ was determined by iron analysis as previously described.[37]

High performance liquid chromatography (HPLC) with detection by tandem mass spectrometry (LC−MS/MS) was conducted on an Agilent Technologies (Santa Clara, CA) 1200 system coupled to an Agilent Technologies 6410 QQQ mass spectrometer. The system was operated with the associated MassHunter software package, which was also used for data collection and analysis.

S-Adenosyl-L-methionine (SAM) and 1-^{13}C SAM were synthesized from ATP and Met or ATP and 1-^{13}C Met, respectively, and purified as described previously.[38] *E. coli* flavodoxin (Flv) and flavodoxin reductase (Flr) were also purified as described previously.[39]

Cloning of the *Streptomyces laurentii tsrM* Gene. The *tsrM* gene from *Streptomyces laurentii* was amplified from a plasmid encoding TsrM using the polymerase chain reaction (PCR).[18] The forward primer, 5′-CGC GGC GTC GAA GAC GC**A GGT** ATG CTC CGT AAA GGC ACC GTC GCT CTG ATC AAC C-3′,

DOI: 10.1021/jacs.5b12592
J. Am. Chem. Soc. 2016, 138, 3416−3426

contained a nine-base GC clamp, a *Bbs*I restriction site (underlined) that results in a four-base 5′ overhang (bolded) when cleaved with *Bbs*I, and the first 34 bases of the *tsrM* gene. The reverse primer, 5′-CGC GGC GTC GAA GAC GC**T CGA** GTC ACC GGA CGG CCT CCG CGA GCT CC-3′, included a nine-base GC clamp, a *Bbs*I restriction site (underlined) resulting in an *Xho*I 5′ overhang upon cleavage (bolded), and the last 25 bases of the *tsrM* gene. The PCR product was isolated and digested with *Bbs*I. In a similar manner, the plasmid, pSUMO, was digested with *Bsa*I and *Xho*I, which generates compatible overhangs. The *tsrM* gene was then ligated into pSUMO to generate a construct that encodes a TsrM fusion to the C-terminus of SUMO, which contains an N-terminal hexahistidine (His_6) tag. The correct DNA sequence was verified at the Penn State Genomics Core Facility (University Park) and designated pSUMO-TsrM.

Overexpression of the *tsrM* Gene. The plasmid pSUMO-TsrM was transformed into the RosettaBlue (DE3) pLysS strain of *E. coli* together with the pDB1282 plasmid encoding the *isc* operon from *Azotobacter vinelandii* to allow for expression in the presence of Fe/S cluster assembly proteins as previously described.[39] A starter culture was inoculated from a single colony and incubated for 24 h at 37 °C while shaking at 250 rpm. Bacterial growth was carried out at 37 °C in 16 L of ethanolamine M9 minimal media that was supplemented with OHCbl (1.3 μM) and allowed to shake at 180 rpm.[40] At an optical density at 600 nm (OD_{600}) of ∼0.3, expression of the genes encoded on pDB1282 was induced with 0.1% (w/v) of L-arabinose while also adding 25 μM $FeCl_3$ and 150 μM Cys. At an OD_{600} of ∼0.55, the flasks were placed on ice for 20 min prior to induction with 800 μM IPTG and additional $FeCl_3$ (25 μM) and Cys (150 μM). Cultures were incubated for 16 h at 20 °C before the cells were collected by centrifugation at 7000*g* for 12 min. On average, two 16 L growths (32 L total) yielded 50 g of cells, which was used for the purification of TsrM.

TsrM containing ^{57}Fe for Mössbauer spectroscopy was overproduced in a similar fashion, except that $^{57}FeCl_3$ was added to a final concentration of 15 μM, and Cys was added to a final concentration of 150 μM.

Purification of TsrM. All purification steps and subsequent manipulations of TsrM were performed in a Coy anaerobic chamber. Cell paste (50 g) was resuspended in 150 mL lysis buffer (50 mM HEPES, pH 7.5, 300 mM KCl, 5% glycerol, 10 mM BME, 10 mM imidazole) with lysozyme (1 mg/mL), DNase (0.1 mg/mL), and OHCbl (0.2 mg/mL) for 30 min at room temperature and then cooled to 4 °C before lysing. Cells were lysed by sonication and centrifuged at 45 000*g* for 1 h to separate insoluble material. The resulting supernatant was loaded onto a pre-equilibrated column of Ni-NTA resin and purified by immobilized-metal affinity chromatography (IMAC). The resin was washed with 200 mL of wash buffer (50 mM HEPES, pH 7.5, 300 mM KCl, 5% glycerol, 10 mM BME, 20 mM imidazole) before eluting with elution buffer (50 mM HEPES, pH 7.5, 300 mM KCl, 15% glycerol, 10 mM BME, 300 mM imidazole). The protein was collected and concentrated by ultracentrifugation using an Amicon centrifugal filter device (EMD Millipore; Billerica, MA) with a 10 kDa cutoff. The TsrM-SUMO fusion protein was then exchanged into cleavage buffer (50 mM HEPES, pH 7.5, 300 mM KCl, 15% glycerol, 10 mM BME) using a PD-10 column and treated with the SUMO protease, Ulp1, overnight on ice (0 °C) to generate native TsrM. The cleavage reaction was then reapplied to the Ni-NTA resin to capture the SUMO protein and Ulp1 protease along with other proteins that bind nonspecifically to the resin, allowing the untagged TsrM to be collected in the flow-through fraction. TsrM was concentrated and exchanged into gel-filtration buffer (50 mM HEPES, pH 7.5, 300 mM KCl, 15% glycerol, 5 mM DTT) as described in previous steps. Chemical reconstitution of TsrM (see below), when appropriate, was conducted after treatment of the fusion construct with Ulp1, but before adding the cleaved fraction to the Ni-NTA resin.

Chemical Reconstitution of TsrM. Chemical reconstitution of TsrM was conducted in cleavage buffer that was supplemented with BME and HEPES, pH 7.5, to final concentrations of 25 mM and 100 mM, respectively. A 5-fold excess of Na_2S was added to the cleavage buffer, which was immediately followed by addition of a 5-fold excess of $FeCl_3$. The mixture was then placed on ice for 15 min, and then precleaved TsrM and Ulp1 were added to the reconstitution mixture, which was subsequently incubated on ice overnight. The reconstituted protein was centrifuged at 10 000*g* to remove any insoluble material. The supernatant was then reapplied to the Ni-NTA resin as previously described, and the flow through was collected and concentrated. The protein was further purified by size exclusion chromatography on an S-200 column equilibrated in gel-filtration buffer.

Determination of TsrM Concentration. The concentration of TsrM was determined by the Bradford assay using BSA (fraction V) as a standard.[41] By conducting an amino acid analysis as previously described,[42] it was determined that the Bradford assay overestimates the concentration of TsrM by a factor of 1.39.

Quantification of Iron, Sulfide, and Cobalamin. The methods of Beinert et al. were used to determine the amount of iron and sulfide present both in as-isolated and in reconstituted TsrM.[37,43] The amount of cobalamin bound to TsrM was determined by its conversion to dicyanocobalamin using a procedure similar to those previously reported.[44,45] TsrM was added to a solution of 0.1 M potassium cyanide, which was subsequently boiled for 5 min to release the resulting dicyanocobalamin. The concentration of dicyanocobalamin was then determined from its UV−vis spectrum (ε_{367} = 30 800 M^{-1} cm^{-1}).[45] UV−vis spectroscopy was also used to investigate cob(I)alamin, which has a sharp absorption peak at 390 nm (ε_{390} = 24 000 M^{-1} cm^{-1}).[44,45]

Determination of TsrM Activity. All reaction mixtures conducted with saturating concentrations of substrates (vide infra) contained 100 mM HEPES, pH 7.5, 200 mM KCl, 10% glycerol, 1 mM SAM, 1 mM Trp, 0.5 μM TsrM, 100 μM Tyr (internal standard (IS)) and a reducing agent consisting of 1 mM DTT or 25 μM Flv, 10 μM Flr, 1 mM NADPH. When reactions were conducted with varying concentrations of one substrate, the varied concentrations ranged from 0 to 120 μM Trp and 0−300 μM SAM, while the concentration of the fixed substrate was held at 500 μM. Additionally, the concentration of TsrM was decreased to 0.1 μM. All components except Trp were incubated for 10 min at room temperature, and a 20 μL aliquot was removed and mixed with 20 μL of 100 mM H_2SO_4 for an initial (t = 0) time point. The reactions were initiated with Trp, and aliquots were removed at designated times from 0 to 60 min and quenched with acid as described above. Standard curves for product quantification by LC−MS/MS contained 100 μM Tyr and varying concentrations of Trp, SAH, SAM, and MeTrp.

Quantification of Product Formation by LC−MS/MS. Quenched reaction mixtures were separated on an Agilent Zorbax Extend-C18 RRHT column (4.6 mm × 50 mm, 1.8 μm particle size) equilibrated in 90.5% solvent A (0.1% formic acid, pH 2.6) and 9.5% solvent B (methanol). A gradient of 9.5−9.8% solvent B was applied from 0.2 to 3.3 min. Subsequently, a gradient of 9.8−30% solvent B was applied from 3.3 to 4.1 min, which was followed by a gradient of 30−60% solvent B from 4.1 to 4.7 min. The percentage of solvent B was held constant from 4.7 to 5.1 min before it was returned to 9.5% from 5.1 to 5.5 min. The column was allowed to re-equilibrate for 3.2 min under initial conditions before subsequent sample injections. Products were detected (Table S3) using electrospray ionization in positive mode (ESI^+) with multiple reaction monitoring (MRM).

TsrM Deuterium Transfer Assays. Reactions contained the following in a final volume of 160 μL: 100 mM HEPES, pH 7.5, 200 mM KCl, 1 μM TsrM, 0.5 mM SAM, 0.5 mM Trp or Trp-d_8, 1 mM DTT, and 100 μM Tyr (IS). All components except SAM and TsrM were dried under vacuum and redissolved in either H_2O or D_2O and incubated further at room temperature to allow for hydron exchange into N1 of Trp for the corresponding reaction mixture. After 30 min, TsrM (2 μL in H_2O-prepared buffer) was added to each sample, which was subsequently incubated for 10 min. Reactions were initiated with SAM and quenched after 1 h.

Data collection and analysis were conducted as described above, with the following modifications. The column was equilibrated in 90% solvent A (5 mM perfluoroheptanoic acid, 5 mM ammonium formate, pH 3.0) and 10% acetonitrile at a flow rate of 0.4 mL/min. A gradient

DOI: 10.1021/jacs.5b12592
J. Am. Chem. Soc. 2016, 138, 3416−3426

from 10 to 30% acetonitrile was applied from 0 to 8 min. The column was then restored to initial conditions from 8 to 8.5 min and equilibrated for 3.5 min before subsequent sample injections.

Preparation of Electron Paramagnetic Resonance (EPR) Samples. TsrM was diluted to a final concentration of 220 μM for each EPR sample, and all samples were flash-frozen in cryogenic liquid isopentane in an anaerobic chamber. EPR samples were prepared by addition of SAM or Trp to final concentrations of 1 mM and dithionite to a final concentration of 5 mM to the protein solution. Each sample was incubated at room temperature for 5 min after introduction of SAM or Trp and an additional 1 min after addition of dithionite, and then placed in an EPR tube before freezing. The resulting samples were stored in liquid nitrogen prior to analysis.

Continuous-Wave Electron Paramagnetic Resonance (CW-EPR). CW-EPR spectra were acquired on an ESP300 Bruker X-band spectrometer equipped with an ER 4102ST resonator. Temperature was controlled by an ER 4112-HV Oxford Instruments (Concord, MA) variable-temperature helium-flow cryostat. Acquisition and control of experimental parameters was performed using EWWIN 2012 software on an external PC via a GPIB interface.[46] In all experiments, the conversion time and the time constant were 40.96 ms, the modulation amplitude was 5 G, and the microwave (MW) power was 20 mW. Spectra were averaged over 10 scans. For spin quantification, a 256 μM Cu(II)-EDTA standard sample was measured using the same experimental conditions. The spin concentrations were extracted by comparing double-integrals of the corresponding EPR signals.

HYSCORE Spectroscopy. HYSCORE spectra were acquired on a Bruker Elexsys E580 spectrometer equipped with a SuperX-FT microwave bridge and a Bruker EN 4118X-MD4 dielectric ENDOR resonator. Microwave pulses generated by the microwave bridge were amplified using a 1 kW traveling wave tube amplifier (Applied Systems Engineering, model 117x). A cryogenic temperature of 8 K was maintained using an ER 4112-HV Oxford Instruments liquid helium-flow cryostat. Acquisition and control of experimental parameters were performed using Bruker XEPR software. Pulse lengths were set to 8 and 16 ns for $\pi/2$ and π pulses, respectively. The delay between the first two pulses (τ) was set to 132 ns. Measurements were performed using 100 ns starting delay values, 20 ns steps and 200 points in each dimension. A shot repetition time of 500 μs was used.

EPR and HYSCORE Data Analysis. All data analysis was performed using the home-written software "Kazan Viewer" in MatLab.[47] Simulations of EPR spectra were performed using the "pepper" routine from the EasySpin package 4.5.[48] HYSCORE simulations were performed using the "kv_hyscorefd" routine from Kazan Viewer package.

Mössbauer Spectroscopy. ^{57}Fe-labeled TsrM was purified from *E. coli* cells cultured in ^{57}Fe-enriched media and subsequently reconstituted with $^{57}FeCl_3$ as described above. All Mössbauer samples were made with 187 μM TsrM and, when applicable, either 1 mM SAM or 1 mM Trp. All samples were frozen and stored in liquid nitrogen before recording of Mössbauer spectra.

Mössbauer spectra were recorded on alternating constant acceleration Mössbauer spectrometers equipped with either a Janis SVT-400 variable-temperature cryostat (low-field) or a Janis 8TMOSS-OM-12SVT variable-temperature cryostat (high-field). The external magnetic field at the sample was applied parallel to the γ radiation. The quoted Mössbauer isomer shifts are referenced relative to the centroid of the spectrum of α-iron recorded at room temperature. Analysis of Mössbauer spectra was carried out using the spectral analysis program WMOSS (www.wmoss.org, SEE Co., Edina, MN).

Cryoreduction. Cryoreduction of TsrM was conducted at the γ-irradiation facility of the Breazeale nuclear reactor at Penn State University. Frozen Mössbauer and EPR samples were kept in liquid nitrogen and reduced by γ-irradiation using a ^{60}Co source for ~20 h in total. A total dose of 8 MRad was delivered to each sample. Following cryoreduction, samples were stored in liquid nitrogen until spectra were recorded.

Protein-Film Electrochemistry. TsrM was exchanged into electrochemistry buffer (25 mM HEPES, pH 7.5, 300 mM KCl, 5% glycerol and 1 mM DTT) by anaerobic gel-filtration chromatography (AGFC) using a PD-10 column and then concentrated to 450 μM. Premethylated TsrM samples were generated by incubation of 110 μM TsrM with 200 μM dithionite for 1 min to generate cob(I)alamin, followed by addition of 400 μM SAM for 5 min to form methylcobalamin. The reaction was then exchanged into electrochemistry buffer lacking DTT by AGFC and concentrated to 450 μM.

Electrochemical experiments were carried out anaerobically in an MBraun Labmaster glovebox using a PGSTAT 12 potentiostat (EcoChemie). A three-electrode configuration was used in a water-jacketed glass cell. A platinum wire was used as the counter electrode and the reference electrode was a standard calomel electrode. Reported potentials are relative to the standard hydrogen electrode.

Baseline measurements were collected using a pyrolytic graphite edge (PGE) electrode that was polished with 1 μm alumina, rinsed, and placed into a glass cell containing a 10 °C mixed buffer solution (10 mM MES, 10 mM CHES, 10 mM TAPS, 10 mM HEPES), pH 8.0, with 200 mM NaCl. A 3 μL aliquot of 350 μM TsrM was applied directly to the polished PGE electrode surface, removed, and placed back into the buffer cell solution. Experiments with the premethylated form of TsrM were performed in the dark to prevent photolysis. Cyclic voltammograms were collected at 10 °C with a scan rate of 100 mV/s, and electrochemical signals were analyzed by correction of the non-Faradaic component from the raw data using the SOAS package.[49]

RESULTS

Cloning and Overexpression of the tsrM Gene and Purification of *TsrM*. Detailed mechanistic studies of cobalamin-dependent RS methylases have been hindered by their inherent insolubility upon overproduction in *E. coli*. In studies of Fom3, GenK, and PhpK, the enzymes were purified from inclusion bodies, refolded, and their Fe/S and cobalamin cofactors were inserted artificially.[32−34] By contrast, in studies by Pierre et al., TsrM was purified from the soluble crude lysate upon its heterologous overproduction in *E. coli*. However, iron and sulfide content was substoichiometric, even after reconstitution, and turnover was dependent upon the addition of cobalamin to reaction mixtures.[28] Our efforts to reproduce the overproduction and purification of TsrM exactly as described by Pierre et al. were unsuccessful. The protein was overwhelmingly produced as inclusion bodies, and attempts to purify the meager amounts present in the soluble portion of the crude lysate resulted in inhomogeneous (<20% pure) enzyme. We therefore adopted an alternate purification strategy using a genetic construct that produces TsrM fused to the C-terminus of the SUMO protein. A His_6 tag on the N-terminus of SUMO allowed for purification of the construct by IMAC, and cleavage of the SUMO-TsrM fusion construct with the SUMO-specific protease, Ulp1, allowed generation of TsrM with its native N-terminus.[50]

Expression of the *tsrM* gene was conducted in *E. coli* RosettaBlue (DE3) pLysS along with plasmid pDB1282, which encodes genes that are involved in Fe/S cluster biosynthesis in *Azotobacter vinelandii*.[39,42] Gene expression was induced in *E. coli* cultured in M9-ethanolamine minimal media supplemented with OHCbl, which has been suggested to increase cobalamin uptake in *E. coli*.[40] Purification of the SUMO-TsrM fusion protein was conducted in an anaerobic chamber, and SDS-PAGE analysis of the eluted fraction showed the protein (78.2 kDa) to be ~30% pure (Figure S1, column A). Upon cleavage of SUMO from TsrM with Ulp1, the reaction mixture was reapplied to the Ni-NTA resin to capture the His_6-containing SUMO protein and the Ulp1 protease along with other

DOI: 10.1021/jacs.5b12592
J. Am. Chem. Soc. 2016, 138, 3416−3426

proteins that bind nonspecifically to the resin. The native protein (66.1 kDa) was collected in the flow-through and determined to be ~95% pure by SDS–PAGE analysis (Figure S1, column B). The yields of pure protein ranged from 10–20 mg from 32 L of *E. coli* culture.

The UV–vis spectrum of as-isolated TsrM shows features consistent with the presence both of Fe/S clusters and of cobalamin, including the broad absorption between 350 and 600 nm, indicative of the Fe/S cluster, and the distinct feature at 390 nm, suggestive of the presence of cob(I)alamin (Figure 2a). Additionally, the spectrum displays an absorbance

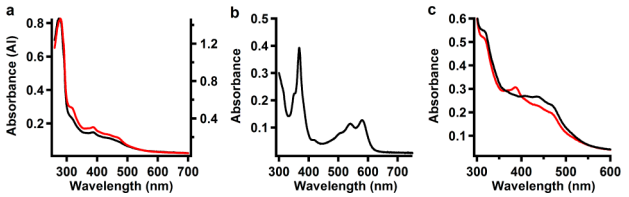

Figure 2. (a) UV–vis spectra of as-isolated TsrM (8 μM, black line, left *y*-axis) and reconstituted TsrM (12 μM, line, right *y*-axis). (b) UV–vis spectrum of as-isolated TsrM (10 μM) treated with potassium cyanide. (c) UV–vis spectra of TsrM (12 μM) before (red line) and after (black line) addition of 300 μM SAM.

maximum at ~280 nm, which contrasts with the previously published UV–vis spectrum of TsrM, which showed a maximum absorbance at 260 nm.[28] Analysis for iron and sulfide showed as-isolated TsrM to contain 3.4 ± 0.4 mol of the former and 3.1 ± 0.2 mol of the latter per polypeptide. After reconstitution, the amount of iron and sulfide changed to 5.0 ± 0.3 and 3.0 ± 0.2 mol, respectively.

To determine the stoichiometry of bound cobalamin, TsrM was treated with potassium cyanide to yield the dicyanocobalamin adduct of cobalamin, which has a strong feature at 367 nm (ε_{367} = 30 800 M^{-1} cm^{-1}). Using the absorbance spectrum shown in Figure 2b along with the molar absorptivity of dicyanocobalamin, TsrM is determined to bind 0.97 ± 0.14 equiv of cobalamin per polypeptide. When SAM is added to reconstituted TsrM, the absorbance peak at 390 nm disappears, suggestive of the methylation of the cob(I)alamin species to give methylcobalamin (Figure 2c). The amount of cob(I)alamin (ε_{390} = 24 000 M^{-1} cm^{-1}) present in as-isolated TsrM was estimated to be ~10% of total cobalamin, which was determined from the ΔA_{390} before and after addition of SAM. Although cob(I)alamin is a supernucleophile and has a low redox potential for the cob(I)alamin/cob(II)alamin couple, it is well known that DTT or BME in the presence of OHCbl can promote the reduction of cob(II)alamin to cob(I)alamin.[51] Therefore, it is not surprising to observe cob(I)alamin in our preparations given that the TsrM lysis buffer contains OHCbl and 10 mM BME and that the protein is purified under strictly anaerobic conditions.

Analysis of Turnover by TsrM. The time-dependent production of MeTrp was quantified by LC–MS/MS. Because dithionite is known to react with cobalamin to form an inactive six-coordinate cobalamin complex,[52] DTT or the flavodoxin reducing system was used to provide external electrons for turnover. While using the flavodoxin reducing system, TsrM exhibited a Michaelis constant (K_M) for SAM of 113.6 μM and a k_{cat} of 34 min^{-1} at saturating concentrations of Trp (Figure 3a), and a K_M for Trp of 11.1 μM and a k_{cat} value of 16 min^{-1} at saturating concentrations of SAM (Figure 3b). Moreover, TsrM

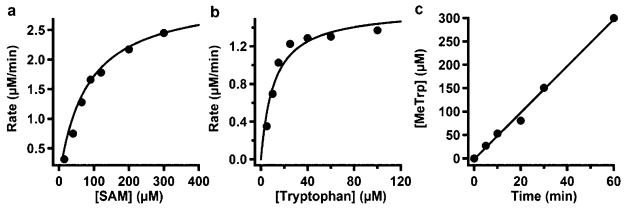

Figure 3. (a) Steady-state kinetic analysis of MeTrp produced by TsrM (0.1 μM) in the presence of (a) 500 μM Trp and varying concentrations of SAM and (b) 500 μM SAM and varying concentrations of Trp. (c) Time-dependent formation of MeTrp by TsrM (0.5 μM) in the presence of 1 mM SAM and 1 mM Trp.

catalyzed ~600 turnovers in 1 h at 25 °C at saturating concentrations of both substrates with the flavodoxin reducing system (Figure 3c), while only completing ~350 turnovers with DTT (Figure S2). These k_{cat} values are much greater than those previously reported for TsrM, which, only after the inclusion of methylcobalamin in the reaction, exhibited a value of 0.26 min^{-1}. However, as reported previously, no 5′-dA was observed during turnover (detection limit <0.1 μM).[28]

TsrM Deuterium Exchange Assay. A review by Zhang et al. suggested a mechanism for TsrM in which a 5′-dA• intermediate initiates substrate-based catalysis by abstracting an H atom from C3 of Trp.[22] Studies by Pierre et al., however, showed that TsrM does not produce 5′-dA during methylation of tryptophan, which might suggest that the reaction does not proceed via a 5′-dA• intermediate.[28] However, a subset of RS enzymes generates a 5′-dA• reversibly, reforming SAM at the end of each turnover.[30] In this instance, deuterium might be expected to accumulate at C-5′ of SAM or SAH when the reaction is conducted using Trp-d_8. Figure 4a shows an LC–MS analysis of products formed by TsrM in the presence of Trp-d_8. Confirming the results of a previous report,[53] the $[M + H]^+$ ion of MeTrp displays an *m/z* of 226.3 (Figure 4a), a mass increase of 7 Da compared to unlabeled MeTrp, indicating that

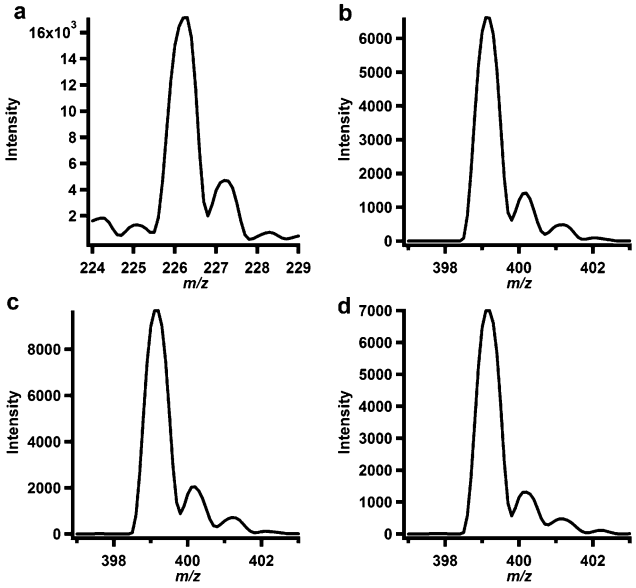

Figure 4. MS analysis of products formed by TsrM. (a) MS analysis of MeTrp formed with Trp-d_8. Mass to charge ratio of SAM after ~300 turnovers of TsrM reaction in (b) H_2O, (c) D_2O, or (d) with Trp-d_8. All reactions contained 0.5 mM SAM, 0.5 mM Trp or Trp-d_8, 1 mM DTT, and 1 μM TsrM.

DOI: 10.1021/jacs.5b12592
J. Am. Chem. Soc. 2016, 138, 3416–3426

C2 and N1 are the only sites where H atom abstraction can occur. To determine whether the 5′-dA● abstracts an H atom from N1 or C2 of Trp and subsequently recombines with methionine to reform SAM, a reaction with Trp-d_8 and a reaction using unlabeled Trp but performed in D_2O were monitored for deuterium enrichment into SAM or SAH by LC−MS. In these reactions, analysis was conducted after TsrM had undergone ∼300 turnovers, wherein ∼60% of SAM had been converted to SAH. Shown in Figure 4 is the isotopic distribution of SAM after a 60 min reaction in both H_2O (Figure 4b) and D_2O (Figure 4c) as well as for the reaction using Trp-d_8 substrate (Figure 4d). The results show that the isotopic distribution of SAM ($[M]^+$ = 399.1) for a control reaction conducted in H_2O is nearly identical to that of a reaction conducted in D_2O as well as that of a reaction using Trp-d_8 as the substrate. Similarly, no enrichment of deuterium into SAH ($[M + H]^+$ = 385.1) is observed in any of the three reactions (Figure S3). These results further support previous conclusions that the 5′-dA● is not used to activate tryptophan during catalysis by TsrM.[53]

Analysis of TsrM by Mössbauer Spectroscopy. The 4.2-K/53-mT Mössbauer spectrum of reconstituted TsrM in the absence of added Trp or SAM is shown in Figure 5. It consists

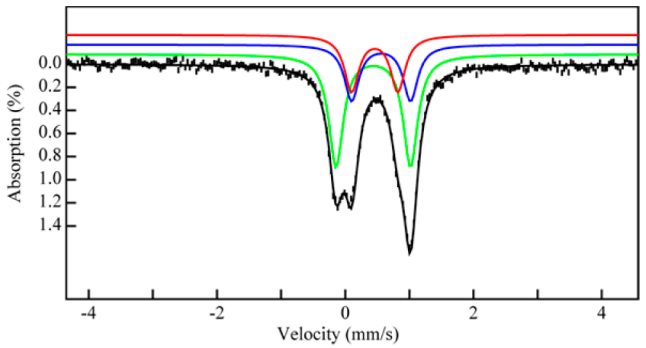

Figure 5. 4.2-K Mössbauer spectrum of reconstituted TsrM recorded in an externally applied field of 53 mT oriented parallel to the gamma beam (vertical bars). The solid black line overlaying the experimental spectrum is the theoretical simulation using parameters quoted in the text. The individual contributions from the valence-delocalized $(Fe^{2.5+})_2$ pair and the high-spin Fe^{2+} and high-spin Fe^{3+} of the partially valence-localized Fe pair are shown in green, blue, and red, respectively.

of two main features, in which the low-energy line at ∼0 mm/s is partially resolved into two peaks, indicating the presence of at least two quadrupole doublets with different parameters, while the high-energy line displays a pronounced shoulder at ∼0.8 mm/s. These spectral characteristics contrast with those typically observed for RS enzymes, wherein only one (typically asymmetric) quadrupole doublet is observed in the absence of SAM.[54] Analysis of the relative intensities of these features (see SI text and Figure S4a) suggests that the spectrum can be described as a superposition of three quadrupole doublets in a 2:1:1 intensity ratio. Of the two solutions (see SI text and Figure S4b,c), we favor the one in which the major quadrupole doublet has parameters typical of $[4Fe-4S]^{2+}$ clusters (δ = 0.44 mm/s and ΔE_Q = 1.16 mm/s, 48% of total intensity, green line). The two minor quadrupole doublets have parameters (δ = 0.56 mm/s and ΔE_Q = 0.92 mm/s, 24% of total intensity, blue line, and δ = 0.46 mm/s and ΔE_Q = 0.72 mm/s, 24% of total intensity, red line) that suggest the presence of an exogenous molecule bound to the unique Fe site of a $[4Fe-4S]^{2+}$ cluster, resulting in a partially valence-localized Fe^{2+}/Fe^{3+} pair.[55−60] The assignment of the features to a $[4Fe-4S]^{2+}$ cluster is further supported by the following observations. First, a spectrum recorded in an 8-T externally applied magnetic field reveals that the cluster has a diamagnetic (S = 0) electron spin ground state (Figure S6). Second, cryoreduction of the sample at 77 K leads to the appearance of features consistent with those of a $[4Fe-4S]^+$ cluster with an S = 1/2 ground state (Figure S7). Given that this sample contains 5.0 Fe per polypeptide, as-isolated TsrM is calculated to contain 1.2 ± 0.1 $[4Fe-4S]^{2+}$ clusters. The spectrum of TsrM in the presence of 1 mM added Trp does not exhibit marked differences from that of as-isolated TsrM in the absence of added substrates (Figure S8). The spectrum of TsrM in the presence of 1 mM SAM exhibits small, yet noticeable, differences from the other two spectra, which is consistent with SAM binding directly to, or in close proximity to, the [4Fe−4S] cluster (Figure S9). However, the perturbation upon addition of SAM is less pronounced than that observed for other RS enzymes.[55−60] As detailed below, HYSCORE experiments rule out direct SAM binding to the cluster.

Analysis of TsrM by CW-EPR. EPR spectroscopy was used to investigate the coordination environment of cob(II)alamin and the electronic properties of the Fe/S cluster in TsrM in the absence and presence of substrates. The EPR spectrum of as-isolated TsrM at 70 K (Figure 6 **Ia**) is best simulated (Figure 6

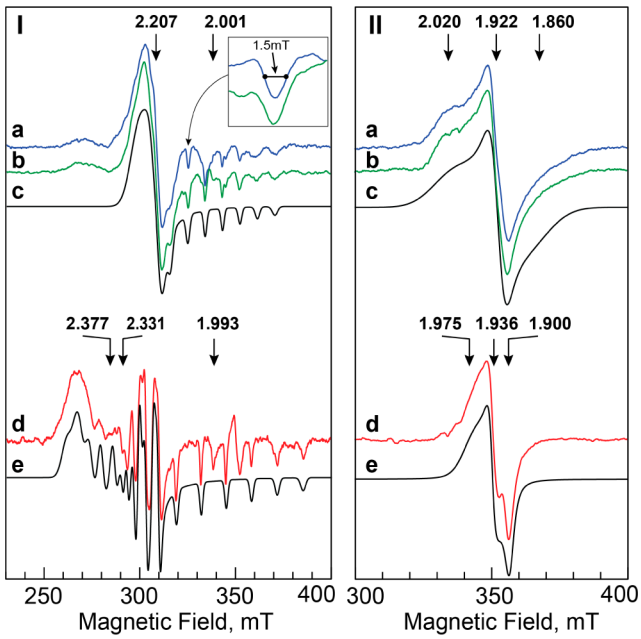

Figure 6. X-band EPR spectra of TsrM. (I) Cob(II)alamin signal of (a) as-isolated TsrM (220 μM) at 70 K in the presence of (b) 1 mM Trp and (d) 1 mM SAM. (II) (a) Reconstituted TsrM (220 μM) at 10 K in the presence of 5 mM dithionite with (b) 1 mM Trp and (d) 1 mM SAM. All black lines (c and e in each panel) are simulations associated with corresponding spectra (see Table 1 for parameters).

Ic) with g-values and ^{59}Co hyperfine coupling constants that are similar to those of typical base-on cob(II)alamin (Table 1).[61] However, the lack of superhyperfine coupling from ^{14}N (I = 1) indicates that neither the cofactor's dimethylbenzimidazole moiety (base-on) nor a histidine ligand (His-on) is coordinated to the cobalt ion, as has been recently reported for an epoxide

DOI: 10.1021/jacs.5b12592
J. Am. Chem. Soc. 2016, 138, 3416−3426

Table 1. Spin Hamiltonian Parameters Used for Simulating EPR Spectra in Figure 6[a]

sim.	g_x	g_y	g_z	^{59}Co HFCc, MHz A_x	A_y	A_z	LW mT
Ic	2.207 (0.052)	2.207 (0.022)	2.001 (0.000)	18 (30)	18 (30)	256 (21)	1.9
Ie	2.377 (0.022)	2.331 (0.022)	1.993 (0.000)	215 (31)	184 (30)	365 (19)	1.9
IIc	2.020 (0.110)	1.922 (0.016)	1.860 (0.100)	–	–	–	4.0[b]
IIe	1.975 (0.050)	1.936 (0.005)	1.901 (0.009)	–	–	–	3.0[b]

[a]Numbers in brackets are FWHH of Gaussian distributions (Strains) used in conjunction with the corresponding constant. [b]A Lorentzian unitary lineshape was used in this simulation instead of a Gaussian lineshape.

reductase and a pair of reductive dehalogenases.[62−64] When Trp is added to the sample, no changes in the spectrum are observed (Figure 6 **Ib**). By contrast, when SAM is added to the sample, the spectrum changes markedly to one that is consistent with cob(II)alamin in its five-coordinate base-off form (Figure 6 **Id**).[65] Double integration of the spectra of cob(II)alamin presented in Figure 6 I correspond to ∼20% of the total sample concentration (40−50 μM spin per 220 μM sample). The EPR data suggest that cob(II)alamin of as-isolated TsrM is five-coordinate and most likely binds a water molecule, and upon addition of SAM, is converted to a pseudo four-coordinate cob(II)alamin, as is observed in the H759G variant of methionine synthase.[66] These spectral perturbations are reminiscent of those observed in methionine synthase, wherein the cobalamin cofactor undergoes similar changes at different stages in the catalytic cycle.[67] In all instances, when the low-potential reductant, dithionite, is added to the samples, the cob(II)alamin signal at 70 K is lost, indicative of reduction of cob(II)alamin to cob(I)alamin (Figure S10), while a new signal appears that is best observed at ∼10 K.

The spectrum shown in Figure 6 **IIa**, recorded at 10 K, is that of reconstituted TsrM in the presence of dithionite. The spectral envelope and the temperature behavior (not observed above 50 K) of the EPR signal are characteristic of $[4Fe-4S]^+$ clusters. Addition of Trp (Figure 6 **IIb**) to the dithionite-reduced sample results in no changes in the EPR spectrum; however, the addition of SAM (Figure 6 **IId**) induces formation of an uncharacteristic $[4Fe-4S]^+$ cluster EPR spectrum, in which all three principal g-values are less than g_e = 2.0023. Simulations of the spectra with (Figure 6 **IIe**) and without SAM (Figure 6 **IIc**) reveal g-values of 1.975, 1.936, and 1.901, and 2.020, 1.922, and 1.860 (Table 1), respectively. While the latter set of g-values do fall in the range that is typical for $[4Fe-4S]^+$ clusters, the g-values for the spectrum in the presence of SAM are very unusual. There are only a few reported cases of a $[4Fe-4S]^+$ cluster that exhibits such an unusual **g**-matrix, such as glyceraldehyde 3-phosphate oxidoreductase[68] and NADH-reduced glutamate synthase.[69] In both cases, these unusual spectra were observed in the presence of additional paramagnetic species. Therefore, our observations may point to a spin−spin interaction of the $[4Fe-4S]^{1+}$ cluster with another undetermined EPR-silent paramagnetic species. For the reasons presented below, we disfavor the direct binding of SAM to the $[4Fe-4S]$ cluster, and thus it is unlikely that this molecule has a direct effect on the electronic structure of the $[4Fe-4S]$ cluster as is found in some other radical SAM enzymes.[31]

Analysis of TsrM by HYSCORE Spectroscopy. Hoffman, Broderick, and co-workers have shown that ^{14}N and ^{13}C hyperfine interactions can be used to pinpoint the binding mode of SAM to the unique Fe site of a $[4Fe-4S]$ cluster.[70] Given the perturbation both of Mössbauer and of EPR spectra upon SAM binding to TsrM, HYSCORE spectroscopy was used to assess whether SAM binds in contact with the Fe/S cluster of TsrM in the same manner observed in other RS enzymes. [1-^{13}C]-SAM was mixed with TsrM and introduced into an EPR tube before being frozen in cryogenic isopentane. Because we were only able to reduce about 10−12% of the $[4Fe-4S]$ cluster using dithionite, the resulting sample was subjected to cryoreduction to generate a concentration of the $[4Fe-4S]^+$ species that was suitable for spectral analysis. Subsequent HYSCORE measurements, however, did not show ^{14}N or ^{13}C signals that would be consistent with SAM binding, although all the resulting spectra did contain "matrix" ^{14}N signals (Figure 7a,b, black arrows) and broad ^{1}H signals (Figure S11) that are typically associated with Cys-ligated $[4Fe-4S]$ clusters. To show the validity of the methods used, similar measurements on dithionite-reduced RlmN were performed, given that SAM binding to the $[4Fe-4S]$ cluster of this enzyme has been established by X-ray crystallography.[71] As can be seen in Figure 7c, the HYSCORE spectrum of the $[4Fe-4S]^+$ cluster of SAM-bound RlmN shows a complex set of signals that can be attributed to coupling with an ^{14}N nucleus. In addition, a ridge is observed around the ^{13}C Larmor frequency (3.6 MHz). The spectral spread of the ^{14}N and ^{13}C signals is very similar to

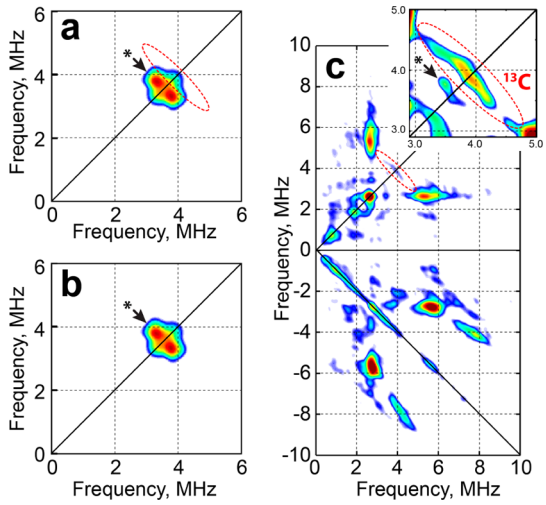

Figure 7. X-band HYSCORE spectra of cryoreduced TsrM in the presence of (a) [1-^{13}C]-SAM and (b) unlabeled SAM, and of (c) dithionite-reduced RlmN in the presence of 1-^{13}C-labeled SAM. Only the low frequency region is shown (see Figure S11 for complete spectra). Black arrows with asterisks indicate matrix ^{14}N signals; red dashed lines depict the expected position of the ^{13}C signal. The insert in (c) shows the enhanced ^{13}C signal found in RlmN (color map levels were lowered to 50%). Experimental conditions: magnetic field, (a, b) 357.5 mT (c) 359.5 mT; microwave frequency, (a,b) 9.685 GHz, (c) 9.707 GHz.

DOI: 10.1021/jacs.5b12592
J. Am. Chem. Soc. 2016, 138, 3416−3426

that published previously for SAM bound to a $[4Fe-4S]^{+}$ cluster (Figure 7c).[70]

Therefore, based on these experiments we conclude that SAM does not directly coordinate the [4Fe−4S] cluster in TsrM. Consequently, we suggest that the differences observed in the $[4Fe-4S]^{+}$ cluster EPR and $[4Fe-4S]^{+}$ cluster Mössbauer signals in the presence and absence of SAM might be due to a perturbation of the local environment of the cluster. HYSCORE measurements on cryoreduced TsrM in the presence of Trp also did not show any signs of Trp binding to the [4Fe−4S] cluster (Figure S11).

Protein Film Electrochemistry of TsrM. TsrM non-covalently adsorbed on PGE electrodes displays two redox couples by cyclic voltammetry (Figure 8a). One quasi-reversible

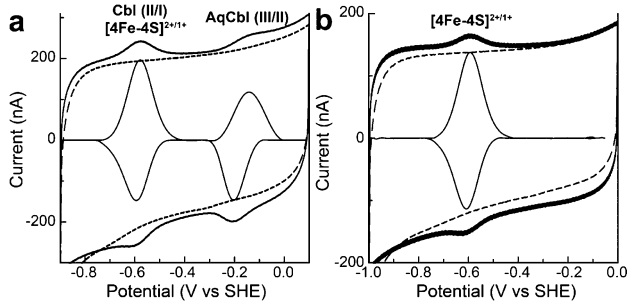

Figure 8. PFE response of TsrM. (a) The as-isolated TsrM (pH 8, 100 mV/s, 10 °C) yields two distinct redox couples, while (b) Premethylated TsrM shows a single species (identical conditions).

feature exhibits a midpoint potential of −550 mV while the other has a midpoint potential of −140 mV (Figure 8a). Because of the observations made by EPR and UV−vis spectroscopies indicating that cobalamin is present as a mixture of states, a predominantly methylcobalamin form of TsrM was generated by first reducing the protein with dithionite for 1 min and then incubating the reduced protein with SAM for 1 min. To ensure that methylation of cobalamin occurred, the reaction was monitored by UV−vis spectroscopy (Figure S12). After addition of dithionite, an increase in absorption at 390 nm was observed, corresponding to cob(I)alamin formation, and only after addition of SAM did this absorption decrease, with a new increase in absorption at 450 nm. This increase in absorption is consistent with formation of methylcobalamin with neither histidine nor dimethylbenzimidazole ligation in the lower-axial position.[72] This observation is consistent with the same conclusion drawn from EPR spectroscopy about the coordination geometry of the cob(II)alamin form of the enzyme. To remove excess SAM and dithionite, the reaction was exchanged into gel-filtration buffer lacking DTT by AGFC. We presume that a methylcobalamin form of TsrM may not be tractable for study by PFE, because methylcobalamin itself would not be amenable to a reversible reduction.[73] However, the methylcobalamin-containing form of TsrM shows a single reversible feature at −560 mV by PFE (Figure 8b), evocative of recent results on the electrochemistry of the RS enzyme, BtrN.[74] Currently, our model is that the −140 mV feature shown in Figure 8a represents a hydroxy/aquo-cobalamin (III/II) couple, while the feature at −550 mV is likely the [4Fe−4S] cluster with a possible contribution from the cobalamin (II/I) redox couple. We note that the potential for the TsrM [4Fe−4S] cluster is consistent with previously reported potentials for one of the [4Fe−4S] clusters in BtrN and the [4Fe−4S] cluster in lysine 2,3-aminomutase.[74,75]

DISCUSSION

The study of radical-dependent strategies for methylating inert carbon centers is an important and growing area of enzymology and chemical biology, and all known enzymes that manifest this activity are members of the RS superfamily. Recently, RS methylases have been grouped into four classes.[22,23] Class A enzymes, represented by RlmN and Cfr, use two cysteines to catalyze the synthesis of a methyl group on C8 and/or C2 of adenosine 2503 of 23S rRNA, an sp^2-hybridized carbon center. Class B enzymes contain cobalamin-binding motifs and catalyze the methylation of both sp^2- and sp^3-hybridized carbon centers. Class C enzymes share sequence homology with HemN, an RS coproporphyrinogen III oxidase, and have been suggested to use two simultaneously bound SAM molecules to catalyze the methylation of sp^2-hybridized carbon centers in several complex natural products. Lastly, unlike class A, B, and C enzymes, class D enzymes, one of which has been shown to catalyze the methylation of 7,8-dihydro-6-hydroxymethylpterin during the biosynthesis of methanopterin, have been suggested to use methylenetetrahydrofolate as the source of the methyl carbon rather than SAM.[76]

The study of RS methylases has been challenging due to the complex substrates on which they operate (rRNA, tRNA, complex natural products), and in many instances, the poor solubility of the enzymes, which has hampered the study of the cobalamin-dependent methylases in particular. In fact, in three of the earliest studies of cobalamin-dependent methylases, the enzymes were purified from inclusion bodies and then reconstituted with iron, sulfide, and cobalamin.[32−34] By contrast, TsrM has proven more tractable for mechanistic dissection, because it operates on a simple substrate and can be isolated in soluble form without the need for refolding. Nevertheless, in our hands, the isolation of the enzyme by conventional IMAC led to enzyme of modest purity, although robust turnover could be demonstrated. Similar results were obtained using the strains and growth and purification conditions outlined by Pierre et al.[28] We therefore developed an alternative strategy for isolating TsrM by generating a DNA construct that encodes a TsrM-SUMO fusion. Initial purification was conducted by IMAC using the His_6-tag at the N-terminus of SUMO, and further purification took advantage of the target protein's inability to bind to the IMAC resin upon reapplication of the Ulp1-cleaved reaction onto the resin. To enhance cobalamin content of the as-isolated enzyme, TsrM was overproduced in *E. coli* cultured in M9-ethanolamine media, which has been suggested to augment cobalamin uptake due to the requirement for adenosylcobalamin by ethanolamine ammonia lyase.[40] Using these procedures, TsrM was purified to ≥95% homogeneity, although the yields were still modest. Nevertheless, the purified and reconstituted protein exhibited a maximum absorbance at 280 nm and other features that are consistent with the presence of both cobalamin and Fe/S clusters.

Biochemical analyses indicate that TsrM, overproduced and isolated as described herein, contains a full complement of bound cobalamin and almost a full complement of [4Fe−4S] clusters. The reconstituted enzyme exhibits a k_{cat} value of 16−30 min^{-1}, which is significantly higher than that previously reported,[28] and unlike the enzyme preparation studied by

DOI: 10.1021/jacs.5b12592
J. Am. Chem. Soc. 2016, 138, 3416−3426

Pierre et al., the activity of TsrM isolated in this study is independent of added cobalamin.

The Mössbauer spectra of TsrM confirm the presence of a $[4Fe-4S]^{2+}$ cluster with a diamagnetic ground state, but the parameters are slightly different than those of $[4Fe-4S]^{2+}$ clusters in other RS enzymes. The 4.2-K/53-mT Mössbauer spectrum suggests the presence of three quadrupole doublets in a 2:1:1 intensity ratio, wherein the major species results from a valence-delocalized $Fe^{2.5+}/Fe^{2.5+}$ pair and the two minor species result from a partially valence-localized Fe^{2+}/Fe^{3+} pair. It is worth mentioning that the isomer shift of 0.46 mm/s, assigned to the Fe^{3+}-like site of the (partially) valence-localized pair, is slightly higher than those typically observed for a high-spin Fe^{3+} ion in a tetrahedral environment of sulfur (0.25−0.30 mm/s); the higher isomer shift might indicate a higher coordination number and/or binding of a ligand with hard O/N ligands.[53,77] Taken together, these parameters are similar to those obtained for [4Fe−4S] clusters that contain an exogenous ligand to one of the iron ions.[55] The binding of Trp to TsrM does not affect the Mössbauer spectrum of the protein to any significant extent; however, the binding of SAM to the protein does lead to small spectral perturbations.

Given that SAM binds to the unique iron site of all previously studied RS proteins, as well as the results of our Mössbauer analysis of TsrM that suggest the presence of a bound ligand to the Fe/S cluster, we assessed whether SAM binds in contact with the Fe/S cluster of TsrM by HYSCORE spectroscopy. We found that neither the amino nor carboxylate groups of SAM or Trp bind directly to the Fe/S cluster. The HYSCORE spectrum of TsrM also suggests that if an endogenous ligand is bound to the cluster, contacts to the cluster are not made through nitrogen atoms. At present we cannot exclude the possibility that other functional groups on SAM (e.g., the 2′ and/or 3′ hydroxyl groups) might coordinate to the cluster. Nevertheless, our results are consistent with biochemical studies of Pierre et al. that showed that a triple variant of TsrM that lacks the cysteines that coordinate the Fe/S cluster can still catalyze the conversion of SAM to SAH, albeit at a slower rate, suggesting that the [4Fe−4S] cluster is not required directly for this catalytic activity.[28]

We used EPR spectroscopy to probe the nature of the cobalamin cofactor of TsrM. The cobalt ion of cobalamin can exist in three different oxidation states: + 1, + 2, and +3. The +2 oxidation state (d^7) has an $S = 1/2$ ground state and is therefore observable by EPR, while the +1 and +3 oxidation states have integer spin ($S = 1$) or zero spin ($S = 0$) ground states, respectively, and are EPR-silent. As-isolated TsrM exhibits an EPR spectrum at 70 K that is consistent with a five-coordinate cob(II)alamin species that contains the unpaired electron in a $3d_{z^2}$ orbital. The absence of superhyperfine splittings from nitrogen nuclei, however, indicate that neither the benzimidazole group of the cofactor nor any other nitrogen atom (e.g., from a histidine residue) is coordinated to the cobalt ion in an axial position, as is observed in some cobalamin-dependent enzymes.[78,79] The addition of Trp has no effect on the EPR spectrum. However, the addition of SAM induces a dramatic change in the spectral envelope that is consistent with a pseudo four-coordinate spectrum seen in cobalamin enzymes. These changes in coordination of the cobalt ion of cobalamin are reminiscent of those observed in methionine synthase, wherein the coordination geometry of cob(II)alamin regulates its reduction to cob(I)alamin by flavodoxin.[80] We hypothesize that SAM binding to TsrM triggers formation of pseudo four-coordinate cob(II)alamin, which upon reduction, generates the cob(I)alamin supernucleophile that attacks the methyl group of SAM during methyltransfer, as has been detailed in the well-studied methionine synthase. At present, the identity of the ligand to the cobalt ion in the five-coordinate cob(II)alamin species is unknown. However, our EPR data suggest that the ligand does not contain nitrogen at the coordinating position. Similar to recent examples of cobalamin-dependent dehalogenases, we predict that the ligand is a water molecule.[63,64]

Studies by Pierre et al.,[28] as well as our studies herein, have shown that the methyl group added to C2 of Trp is derived from SAM; however, no net generation of 5′-dA is observed. In our studies, we also probed for the possibility that SAM might undergo a reversible reductive cleavage by assessing whether C-5′ of SAH or SAM is enriched in deuterium when the reaction is conducted with Trp-d_8 or in D_2O. No deuterium enrichment was observed, suggesting that the reversible reductive cleavage does not occur in TsrM.

Our studies herein, and previous studies by Pierre et al.,[28] therefore raise the question: What defines an RS enzyme? The classical RS enzyme is described by pfam04055, which is now composed of almost 114 000 individual sequences.[29] It consists of an RS domain containing a partial (α_6/β_6) or full (α_8/β_8) triose-phosphate isomerase barrel that houses binding determinants for the [4Fe−4S] cluster and SAM, with the cysteines that coordinate the [4Fe−4S] cluster most often occurring in a compact CxxxCxxC motif. To date, TsrM is the only enzyme of pfam04055 to be rigorously shown not to catalyze the reductive cleavage of SAM to give a 5′-dA•. Interestingly, PhnJ[81] and ThiC,[82] two enzymes that catalyze formation of a 5′-dA• intermediate, are not members of pfam04055, nor is Dph2, which catalyzes formation of a 3-amino-3-carboxypropyl radical.[83,84] These enzymes, unlike TsrM, are structurally distinct (or predicted to be) from those of pfam04055. Although our work details steps associated with methylation of cobalamin by SAM, the mechanism by which the methyl group is transferred to C2 of Trp has not been elucidated.[52] It will be gratifying to understand the raison d'être for using an RS enzyme to catalyze a reaction that does not require reductive cleavage of SAM.

■ ASSOCIATED CONTENT

Supporting Information

The Supporting Information is available free of charge on the ACS Publications website at DOI: 10.1021/jacs.5b12592.

Experimental methods, additional figures and spectral analyses. (PDF)

■ AUTHOR INFORMATION

Corresponding Authors

*alexey.silakov@gmail.com
*elliott@bu.edu
*ckrebs@psu.edu
*squire@psu.edu

Notes

The authors declare no competing financial interest.

■ ACKNOWLEDGMENTS

We thank Candace Davison of the Radiation Science & Engineering Center at the Breazeale Nuclear Reactor at Penn State for assistance in carrying out cryoreduction experiments. We thank Erica Schwalm (Pennsylvania State University) for

DOI: 10.1021/jacs.5b12592
J. Am. Chem. Soc. 2016, 138, 3416−3426

providing the RlmN that was used for HYSCORE spectroscopy, and Dr. Thomas Brunold (University of Wisconsin, Madison) for helpful discussions. This work was supported by NIH grants GM-103268 (SJB and CK), GM-101957 (SJB), and GM-090327 (WLK), as well as NSF grant MCB-1122977 (SJE).

REFERENCES

(1) Booker, S. J. *Curr. Opin. Chem. Biol.* **2009**, *13*, 58.
(2) Challand, M. R.; Driesener, R. C.; Roach, P. L. *Nat. Prod. Rep.* **2011**, *28*, 1696.
(3) Frey, P. A.; Hegeman, A. D.; Ruzicka, F. J. *Crit. Rev. Biochem. Mol. Biol.* **2008**, *43*, 63.
(4) Kudo, F.; Kasama, Y.; Hirayama, T.; Eguchi, T. *J. Antibiot.* **2007**, *60*, 492.
(5) Gomez Macqueo Chew, A.; Bryant, D. A. *Annu. Rev. Microbiol.* **2007**, *61*, 113.
(6) Mao, Y.; Varoglu, M.; Sherman, D. H. *Chem. Biol.* **1999**, *6*, 251.
(7) Ostash, B.; Saghatelian, A.; Walker, S. *Chem. Biol.* **2007**, *14*, 257.
(8) Hidaka, T.; Goda, M.; Kuzuyama, T.; Takei, N.; Hidaka, M.; Seto, H. *Mol. Gen. Genet.* **1995**, *249*, 274.
(9) Kuzuyama, T.; Hidaka, T.; Kamigiri, K.; Imai, S.; Seto, H. *J. Antibiot.* **1992**, *45*, 1812.
(10) Woodyer, R. D.; Shao, Z.; Thomas, P. M.; Kelleher, N. L.; Blodgett, J. A. V.; Metcalf, W. W.; van der Donk, W. A.; Zhao, H. *Chem. Biol.* **2006**, *113*, 1171.
(11) Woodyer, R. D.; Li, G.; Zhao, H.; van der Donk, W. A. *Chem. Commun.* **2007**, *4*, 359.
(12) Nunez, L. E.; Mendez, C.; Brana, A. F.; Blanco, G.; Salas, J. A. *Chem. Biol.* **2003**, *10*, 301.
(13) Marous, D. R.; Lloyd, E. P.; Buller, A. R.; Moshos, K. A.; Grove, T. L.; Blaszczyk, A. J.; Booker, S. J.; Townsend, C. A. *Proc. Natl. Acad. Sci. U. S. A.* **2015**, *112*, 10354.
(14) Kim, J.-Y.; Suh, J.-W.; Kang, S.-H.; Phan, T. H.; Park, S.-H.; Kwon, H.-J. *Biochem. Biophys. Res. Commun.* **2008**, *372*, 730.
(15) Anderle, C.; Alt, S.; Gulder, T.; Bringmann, G.; Kammerer, B.; Gust, B.; Heide, L. *Arch. Microbiol.* **2007**, *187*, 227.
(16) Dairi, T.; Ohta, T.; Hashimoto, E.; Hasegawa, M. *Mol. Gen. Genet.* **1992**, *232*, 262.
(17) Kuzuyama, T.; Seki, T.; Dairi, T.; Hidaka, T.; Seto, H. *J. Antibiot.* **1995**, *48*, 1191.
(18) Kelly, W. L.; Pan, L.; Li, C. *J. Am. Chem. Soc.* **2009**, *131*, 4327.
(19) Rachid, S.; Scharfe, M.; Blöcker, H.; Weissman, K. J.; Müller, R. *Chem. Biol.* **2009**, *16*, 70.
(20) Hidaka, T.; Hidaka, M.; Kuzuyama, T.; Seto, H. *Gene* **1995**, *158*, 149.
(21) Kamigiri, K.; Hidaka, T.; Imai, S.; Murakami, T.; Seto, H. *J. Antibiot.* **1992**, *45*, 781.
(22) Zhang, Q.; van der Donk, W. A.; Liu, W. *Acc. Chem. Res.* **2012**, *45*, 555.
(23) Bauerle, M. R.; Schwalm, E. L.; Booker, S. J. *J. Biol. Chem.* **2015**, *290*, 3995.
(24) Li, C.; Kelly, W. L. *Nat. Prod. Rep.* **2010**, *27*, 153.
(25) Zhou, P.; O'Hagan, D.; Mocek, U.; Zeng, Z.; Yuen, L. D.; Frenzel, T.; Unkefer, C. J.; Beale, J. M.; Floss, H. G. *J. Am. Chem. Soc.* **1989**, *111*, 7274.
(26) Woodard, R. W.; Tsai, M.-D.; Floss, H. G.; Crooks, P. A.; Coward, J. K. *J. Biol. Chem.* **1980**, *255*, 9124.
(27) Hegazi, M. F.; Borchardt, R. T.; Schowen, R. L. *J. Am. Chem. Soc.* **1979**, *101*, 4359.
(28) Pierre, S.; Guillot, A.; Benjdia, A.; Sandström, C.; Langella, P.; Berteau, O. *Nat. Chem. Biol.* **2012**, *8*, 957.
(29) Akiva, E.; Brown, S.; Almonacid, D. E.; Barber, A. E., 2nd; Custer, A. F.; Hicks, M. A.; Huang, C. C.; Lauck, F.; Mashiyama, S. T.; Meng, E. C.; Mischel, D.; Morris, J. H.; Ojha, S.; Schnoes, A. M.; Stryke, D.; Yunes, J. M.; Ferrin, T. E.; Holliday, G. L.; Babbitt, P. C. *Nucleic Acids Res.* **2014**, *42*, D521.
(30) Frey, P. A.; Booker, S. J. *Adv. Protein Chem.* **2001**, *58*, 1.
(31) Broderick, J. B.; Duffus, B. R.; Duschene, K. S.; Shepard, E. M. *Chem. Rev.* **2014**, *114*, 4229.
(32) Allen, K. D.; Wang, S. C. *Arch. Biochem. Biophys.* **2014**, *543*, 67.
(33) Kim, H. J.; McCarty, R. M.; Ogasawara, Y.; Liu, Y.; Mansoorabadi, S. O.; LeView, J.; Liu, H. *J. Am. Chem. Soc.* **2013**, *135*, 8093.
(34) Werner, W. J.; Allen, K. D.; Hu, K.; Helms, G. L.; Chen, B. S.; Wang, S. C. *Biochemistry* **2011**, *50*, 8986.
(35) Goss, R. J.; Newill, P. L. *Chem. Commun.* **2006**, *47*, 4924.
(36) Laemmli, U. K. *Nature* **1970**, *227*, 680.
(37) Beinert, H. *Methods Enzymol.* **1978**, *54*, 435.
(38) Iwig, D. F.; Booker, S. J. *Biochemistry* **2004**, *43*, 13496.
(39) Cicchillo, R. M.; Iwig, D. F.; Jones, A. D.; Nesbitt, N. M.; Baleanu-Gogonea, C.; Souder, M. G.; Tu, L.; Booker, S. J. *Biochemistry* **2004**, *43*, 6378.
(40) Bandarian, V.; Matthews, R. G. *Methods Enzymol.* **2004**, *380*, 152.
(41) Bradford, M. M. *Anal. Biochem.* **1976**, *72*, 248.
(42) Lanz, N. D.; Grove, T. L.; Gogonea, C. B.; Lee, K. H.; Krebs, C.; Booker, S. J. *Methods Enzymol.* **2012**, *516*, 125.
(43) Beinert, H. *Anal. Biochem.* **1983**, *131*, 373.
(44) Ragsdale, S. W.; Lindahl, P. A.; Münck, E. *J. Biol. Chem.* **1987**, *262*, 14289.
(45) Ljungdahl, L. G.; LeGall, J.; Lee, J. P. *Biochemistry* **1973**, *12*, 1802.
(46) *EWWIN 2012 Software Package*; Scientific Software Services, 2012.
(47) Silakov, A.; Epel, B. *Kazan Viewer*; https://sites.google.com/site/silakovalexey/kazan-viewer (accessed July 14 2015).
(48) Stoll, S.; Schweiger, A. *J. Magn. Reson.* **2006**, *178*, 42.
(49) Fourmond, V.; Hoke, K.; Heering, H. A.; Baffert, C.; Leroux, F.; Bertrand, P.; Leger, C. *Bioelectrochemistry* **2009**, *76*, 141.
(50) Marblestone, J. G.; Edavettal, S. C.; Lim, Y.; Lim, P.; Zuo, X.; Butt, T. R. *Protein Sci.* **2006**, *15*, 182.
(51) Jarrett, J. T.; Goulding, C. W.; Fluhr, K.; Huang, S.; Matthews, R. G. *Methods Enzymol.* **1997**, *281*, 196.
(52) Salnikov, D. S.; Silaghi-Dumitrescu, R.; Makarov, S. V.; van Eldik, R.; Boss, G. R. *Dalton Trans.* **2011**, *40*, 9831.
(53) Benjdia, A.; Pierre, S.; Gherasim, C.; Guillot, A.; Carmona, M.; Amara, P.; Banerjee, R.; Berteau, O. *Nat. Commun.* **2015**, *6*, 8377.
(54) Pandelia, M.-E.; Lanz, N. D.; Booker, S. J.; Krebs, C. *Biochim. Biophys. Acta, Mol. Cell Res.* **2015**, *1853*, 1395.
(55) Seemann, M.; Janthawornpong, K.; Schweizer, J.; Böttger, L. H.; Janoschka, A.; Ahrens-Botzong, A.; Tambou, E. N.; Rotthaus, O.; Trautwein, A. X.; Rohmer, M.; Schünemann, V. *J. Am. Chem. Soc.* **2009**, *131*, 13184.
(56) Yang, J.; Naik, S. G.; Ortillo, D. O.; García-Serres, R.; Li, M.; Broderick, W. E.; Huynh, B. H.; Broderick, J. B. *Biochemistry* **2009**, *48*, 9234.
(57) Krebs, C.; Henshaw, T. F.; Cheek, J.; Huynh, B. H.; Broderick, J. B. *J. Am. Chem. Soc.* **2000**, *122*, 12497.
(58) Cosper, M. M.; Jameson, G. N. L.; Davydov, R.; Eidsness, M. K.; Hoffman, B. M.; Huynh, B. H.; Johnson, M. K. *J. Am. Chem. Soc.* **2002**, *124*, 14006.
(59) Lee, K. H.; Saleh, L.; Anton, B. P.; Madinger, C. L.; Benner, J. S.; Iwig, D. F.; Roberts, R. J.; Krebs, C.; Booker, S. J. *Biochemistry* **2009**, *48*, 10162.
(60) Lanz, N. D.; Pandelia, M.-E.; Kakar, E. S.; Lee, K.-H.; Krebs, C.; Booker, S. J. *Biochemistry* **2014**, *53*, 4557.
(61) Stich, T. A.; Buan, N. R.; Brunold, T. C. *J. Am. Chem. Soc.* **2004**, *126*, 9735.
(62) Miles, Z. D.; Myers, W. K.; Kincannon, W. M.; Britt, R. D.; Bandarian, V. *Biochemistry* **2015**, *54*, 4927.
(63) Bommer, M.; Kunze, C.; Fesseler, J.; Schubert, T.; Diekert, G.; Dobbek, H. *Science* **2014**, *346*, 455.
(64) Payne, K. A. P.; Quezada, C. P.; Fisher, K.; Dunstan, M. S.; Collins, F. A.; Sjuts, H.; Levy, C.; Hay, S.; Rigby, S. E. J.; Leys, D. *Nature* **2015**, *517*, 513.

DOI: 10.1021/jacs.5b12592
J. Am. Chem. Soc. 2016, 138, 3416−3426

(65) Liptak, M. D.; Fleischhacker, A. S.; Matthews, R. G.; Telser, J.; Brunold, T. C. *J. Phys. Chem. B* **2009**, *113*, 5245.
(66) Drennan, C. L.; Huang, S.; Drummond, J. T.; Matthews, R. G.; Lidwig, M. L. *Science* **1994**, *266*, 1669.
(67) Matthews, R. G. *Acc. Chem. Res.* **2001**, *34*, 681.
(68) Hagedoorn, P. L.; Freije, J. R.; Hagen, W. R. *FEBS Lett.* **1999**, *462*, 66.
(69) Vanoni, M. A.; Edmondson, D. E.; Zanetti, G.; Curti, B. *Biochemistry* **1992**, *31*, 4613.
(70) Walsby, C. J.; Ortillo, D.; Yang, J.; Nnyepi, M. R.; Broderick, W. E.; Hoffman, B. M.; Broderick, J. B. *Inorg. Chem.* **2005**, *44*, 727.
(71) Boal, A. K.; Grove, T. L.; McLaughlin, M. I.; Yennawar, N. H.; Booker, S. J.; Rosenzweig, A. C. *Science* **2011**, *332*, 1089.
(72) Menon, S.; Ragsdale, S. W. *Biochemistry* **1998**, *37*, 5689.
(73) Pratt, J. M. In *B12*; Dolphin, D., Ed.; John Wiley & Sons: New York, 1982; Vol. *1*, p 325.
(74) Maiocco, S. J.; Grove, T. L.; Booker, S. J.; Elliott, S. J. *J. Am. Chem. Soc.* **2015**, *137*, 8664.
(75) Hinckley, G. T.; Frey, P. A. *Biochemistry* **2006**, *45*, 3219.
(76) Allen, K. D.; Xu, H.; White, R. H. *J. Bacteriol.* **2014**, *196*, 3315.
(77) Münck, E. In *Physical Methods in Bioinorganic Chemistry: Spectroscopy and Magnetism*; Que, L., Jr., Ed.; University Science Books, 2000; p 287.
(78) Banerjee, R.; Ragsdale, S. W. *Annu. Rev. Biochem.* **2003**, *72*, 209.
(79) Liptak, M. D.; Datta, S.; Matthews, R. G.; Brunold, T. C. *J. Am. Chem. Soc.* **2008**, *130*, 16374.
(80) Hoover, D. M.; Jarrett, J. T.; Sands, R. H.; Dunham, W. R.; Ludwig, M. L.; Matthews, R. G. *Biochemistry* **1997**, *36*, 127.
(81) Kamat, S. S.; Williams, H. J.; Raushel, F. M. *Nature* **2011**, *480*, 570.
(82) Chatterjee, A.; Li, Y.; Zhang, Y.; Grove, T. L.; Lee, M.; Krebs, C.; Booker, S. J.; Begley, T. P.; Ealick, S. E. *Nat. Chem. Biol.* **2008**, *4*, 758.
(83) Zhu, X.; Dzikovski, B.; Su, X.; Torelli, A. T.; Zhang, Y.; Ealick, S. E.; Freed, J. H.; Lin, H. *Mol. BioSyst.* **2011**, *7*, 74.
(84) Zhang, Y.; Zhu, X.; Torelli, A. T.; Lee, M.; Dzikovski, B.; Koralewski, R. M.; Wang, E.; Freed, J.; Krebs, C.; Ealick, S. E.; Lin, H. *Nature* **2010**, *465*, 891.

■ NOTE ADDED AFTER ASAP PUBLICATION

This paper was published ASAP on March 3, 2016, with a correction in the Results Section to the discussion of the determination of the stoichiometry of bound cobalamin. The corrected version was reposted on March 7, 2016.

DOI: 10.1021/jacs.5b12592
J. Am. Chem. Soc. 2016, 138, 3416−3426